J. ISSAAS Vol. 26, No. 1: 132-144 (2020)

A PHYSICALLY-BASED MODEL FOR SIMULATING RUNOFF OF LAGAWE RIVER SUB-WATERSHED, IFUGAO, PHILIPPINES

Victorino A. Bato and Eduardo P. Paningbatan, Jr.
Division of Soil Science, Agricultural Systems Institute, College of Agriculture and Food Science, University of the Philippines Los Banos, Laguna, Philippines

(Received: January 23, 2020; Accepted: June 2, 2020)

ABSTRACT

A dynamic, physical model was created to simulate runoff of Lagawe River Sub-watershed. A tipping-bucket rain gauge was installed to gather event-based rainfall data and a water-level recorder was installed on a straight segment of Lagawe River to gather water depth. Land use/land cover data was derived from the image classification of Landsat data. Elevation, slope, and local drainage direction maps were generated from digital elevation model using GIS processing techniques. Manning's equation was utilized to model the velocity of runoff. The maps, rainfall, and water-level data served as input to the physical, dynamic model, which was written using PCRaster language. An R^2 of 0.82 was achieved between the correlation of the measured and predicted streamflow. Also, the t-statistic showed no significant difference between the measured and predicted streamflow. Based on the statistical analyses and indices, the dynamic, physical model was able to simulate runoff and predict streamflow.

Key words: PCRaster, GIS, remote sensing, Lagawe, Ifugao, and Landsat

INTRODUCTION

The FAO (Food and Agriculture Organization) defines a watershed as a geographical area drained by a watercourse (FAO, n.d.). Watershed provides ecosystem services. Healthy watersheds provide valuable services to society, including the supply and purification of fresh water (Postel and Thompson 2005). The Forest Management Bureau of the Philippines classifies watersheds according to their sizes: river basin (>100,000 ha), large watershed (>50,000 ha), medium watershed (>10,000), small watershed (>1,000 ha), and micro watershed (<1,000 ha) (FMB n.d.).

Rain falling within the confines of a watershed enters the soil surface through a process called infiltration. Rain-water in excess of the soil's instantaneous infiltration capacity accumulates in the soil's surface, then flows downslope as surface runoff through various stream channels, until the stream channels converge into one. Ground water flow contributes significantly to streamflow (Frisbee et al. 2011), especially for large watersheds. During rainstorm events, however, surface runoff becomes the major source of streamflow (Wu et al. 2018; Pandey et al. 2008).

Streamflow is the volumetric discharge expressed in volume per unit time (typically cubic feet per second (ft^3/s) or cubic meters per second (m^3/s)) that takes place in a stream or channel and varies in time and space (Wiche and Holmes 2016). Streamflow varies from stream to stream, depending on the physical properties of the watershed or river basin. Wider and deeper channels can convey a higher volume of water than narrower and shallower ones. Streamflow also depends on the physical condition of the stream. Slope, meandering as oppose to straight, and the presence of rocks that increases surface roughness highly affects the flow velocity of water.

Streamflow is the indicator of the overall health of a watershed. Having accurate streamflow data is an important factor in watershed planning and sustainable water resource management (Ravazi and Coulibaly 2013). A healthy watershed should have continuous supply of water even during the dry months. A stream that always dries-up during summer is an indicator that its watershed is not able to store enough water, available through rainfall during the wet season, to maintain its base flow. Such a condition is indicative of the poor or degraded condition of the watershed's vegetative cover and soil.

Accurate prediction of streamflow is an essential ingredient for both water quality and quality management (Mehr et al. 2013). Water quality is associated with soil erosion and runoff; soil erosion and runoff are associated with land use and land cover. Water quality decreases as vegetation cover of a watershed becomes degraded. Increase in urban lands are usually associated with an increase in high streamflow, decrease in low streamflow, and an increased variability in streamflow because of the increased impervious surface caused by urbanization decreases infiltration of precipitation and increases runoff (Tu 2009).

Streamflow data is also used in the design of critical engineering structures, such as highways, drainage systems, and reservoirs (Razavi and Coulibaly 2013). Properly designed bridges, drainage systems, and irrigation canals should be able to handle peak streamflow coming from surface runoff.

Streamflow forecasting and modeling are classified into four categories: conceptual, metric, physics-based, and data-driven (Besaw et al 2010). Conceptual models involves a simplified conceptualization of a hydrologic process. Metric models are based on unit hydrograph theory and are not based on hydrologic processes. Physically-based models involve a detailed interaction of various physical processes controlling the behavior of a system (Wu and Chau 2011). Data driven models are useful for river flow forecasting where the main concern is accurate prediction of runoff without any underlying information on the physics of the hydrological process (He et al. 2014). According to Kuchment et al. (1996), for a runoff model to help solve environmental problems related to the hydrologic cycle, erosion, and water quality, physical process representation and available experimental and observational data should be present.

Physically-based models have the following characteristics and advantages. First, physically-based models have parameters with clear physical meaning. Second, physically-based models can provide satisfactory results if effective values are used for some parameters instead of measured or a priori values. Third, physically-based models provide an opportunity to use simulation to explore different assumptions and hypothesis (Kuchment et al. 1996). The rainfall-runoff process can be influenced by many factors such as weather conditions, land-use and vegetation cover, infiltration, and evapotranspiration (Mehr et al. 2013). Predicting streamflow from surface runoff is complex due to the non-homogenous conditions that exists within the watershed that directly affect the amount of runoff: namely land use/land cover and soil conditions (Yan et al. 2013). However, through numerical simulation, together with weather data and land-related inputs, the surface runoff and streamflow can be modelled.

Runoff and soil erosion are processes that occur in a watershed. Quantification of the volume of runoff is necessary in managing the land use of the watershed and its ability to supply water to a reservoir. Tools such as models are needed by managers to properly assess the condition of the watershed at various times and rainfall conditions. Thus, there is a need to develop a model that could quantify runoff from a watershed based on land use and rainfall for better management of its land use.

This study sought to build a dynamic, physical model that can simulate runoff during rainstorm events using GIS, remote sensing, and sensor technologies. Specifically it sought to (1) gather event-based rainfall data through the installation of a tipping-bucket rain gauge with data recorder, (2) gather

water-level data through the installation of water-level recorder, and (3) build a dynamic physical model using GIS and PCRaster Software.

The model developed in this research can only be used to simulate surface runoff occurring during erosive rainfall events, high intensity and long duration rainfalls. The model was calibrated using such types of data. The model is also designed to work on extreme, rainfall events that occur only once in every ten or twenty years. The model has been tested to work well on small watersheds, but will also work in larger watersheds.

MATERIALS AND METHODS

Study area. The project site is the Lagawe River Sub-watershed located in Ifugao province, Philippines (Fig. 1). The project site lies within the geographic extents of: 121º 5'E – 121º 9'E Longitude and 16º 48'N – 16º 54'N Latitude. The sub-watershed has an approximate area of 7,392 hectares (Bato 2019), based on computation using GIS (Geographic Information Systems) and is classified as a small watershed by the Forest Management Bureau (FMB 2019).

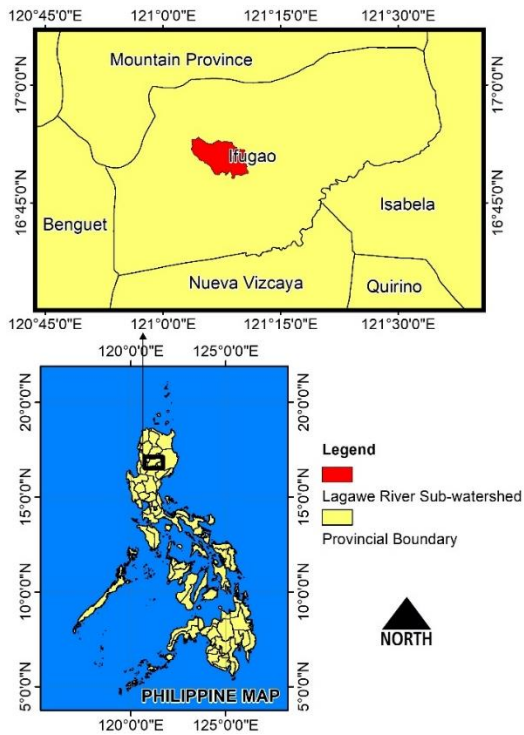

Fig. 1. Location of project area relative to the Philippines.

Installation of tipping-bucket rain gauge. A tipping-bucket rain gauge was installed within the boundary of Lagawe River Sub-watershed in order to record event-based rainfall occurrences (Fig. 2). Each bucket tip is equivalent to 0.2 millimeters of rainfall, every tip is recorded with date and time stamp. Event-based rainfall data is needed as input to the dynamic model. The model required high-temporal-resolution rainfall data to predict streamflow to generate a river hydrograph for rainstorm events. The rain gauge was installed in Barangay Poblacion, Hingyon municipality, Ifugao province. The geographic coordinate of the rain gauge is: 121º 5' 56.46" E, 16 º 51' 8.66" N. The tipping-bucket rain gauge was mounted on ½-inch galvanized pipe attached to the steel beam of the covered stage within the property of the Catholic Church in Hingyon.

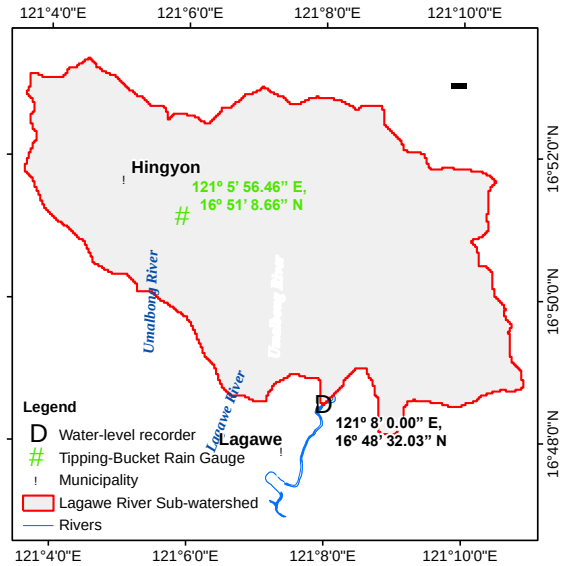

Fig. 2. Location of the tipping-bucket rain gauge and water level recorder installed within Lagawe River Sub-watershed, Ifugao Province.

Installation of capacitive water-level recorder. Water depth was monitored using a capacitive water-level recorder (Fig. 2). Water depth was recorded every five-minutes, together with the date and time of recording. The measured water depth was used to compare and assess the output hydrograph of the model. The water level recorder was installed on a straight segment of the Lagawe River. The water-level recorder was installed on the lower segment of Lagawe River located in Barangay Boliwong, Lagawe municipality, Ifugao province. The geographic coordinate is: 121º 8' 0.00" E, 16º 48' 32.03" N. This water level recorder was encased in a PVC (Polyvinyl Chloride) pipe, with numerous holes, attached to the riprap wall of the river. The PVC pipe provided the water level recorder security from theft and protection from the elements. The holes on the pipe ensured that water can get-in-and-out of the pipe for proper water level recording.

Rain and water-level data collection started May 4, 2015, when the sensors were installed and ended December 17, 2015, when enough erosive rainfall data was gathered.

Data analysis and modelling. During rainstorm events, water normally flows from an area of higher elevation to an area of lower elevation. Water flows through the soil surface as surface runoff or through channels like rills and gullies. The rills and gullies are like river channels that carry surface runoff downslope at a certain velocity. The velocity of surface runoff along these channels can be estimated using Manning's Equation (Equation 1).

$$V = \frac{r^{2/3}\ \alpha^{1/2}}{n} \qquad \textit{(Eq. 1)}$$

Where:

V is velocity, *m/sec*
r is the hydraulic radius, *m*
α is the slope
n is Manning's surface roughness index

Manning's n can be generated by recoding the land use map to create a Manning's Roughness Index Map. The hydraulic radius is the ratio of the cross-sectional area of flow to the wetted perimeter (Equation 2).

$$r = \frac{h \times w}{w + (2 \times h)} \qquad \textit{(Eq. 2)}$$

Where:

r is the hydraulic radius, m
h is the height of flow, m
w is the width of flow, m

Surface runoff travels down the slope at a certain velocity, increasing, as the height of the surface runoff increases, and decreasing, as the surface roughness increases. A uniform sloping surface in a landscape could be assumed as a very wide channel without sides. In such a case, the hydraulic radius, *r*, becomes the height of flow, *h*, (Hillel, 2004). Thus Equation 1 becomes:

$$V = \frac{h^{2/3} \ \alpha^{1/2}}{n} \qquad \textit{(Eq. 3)}$$

Where:

V is velocity, *m/sec*
h is the height of flow, m
α is the slope
n is Manning's surface roughness index

The dynamic, physical model conforms to the water balance equation (Equation 4) in computing for the surface runoff of watersheds.

$$R = P - (I + E) \qquad \textit{(Eq. 4)}$$

Where:

R is surface runoff
P is precipitation
I is infiltration
E is evapotranspiration

During erosive rainfall events, evapotranspiration can be ignored because its rate is very insignificant compared to rainfall intensity. Thus Equation 4 becomes:

$$R = P - I \qquad \textit{(Eq. 5)}$$

Where:

R is surface runoff
P is precipitation
I is infiltration

Infiltration is highly dependent on time, moisture, and land use. During rainy season, the soil is already close to saturation. During rain-storm events, the soil becomes saturated and infiltration is already at its steady-state, which is very close to the saturated hydraulic conductivity.

In a watershed, which is in three-dimension with X, Y, and Z components (longitude, latitude, and elevation or eastings, northings, and elevation), geographic information systems (GIS) will be used to facilitate overlay and map algebra. PCRaster Software will be used for the dynamic, physical modelling because of the following reasons: (1) PCRaster in GIS-based, (2) PCRaster allows the modeler to work and modify equations, and (3) Only PCRaster has the ability to move materials (water) following the LDD (local drainage direction) network in a dynamic manner. Without the LDD it would be impossible to create this model.

Land within the sub-watershed have various land uses. Land use/ land cover of the watershed was derived from the classification of Landsat 8 data (Fig. 3), supplemented by digitizing the location

of rice terraces from Google Maps. From the land use map (Fig. 4h), a Manning's n was assigned to each land use class to generate a Manning's n map (Fig. 4g). This map was one of the inputs of the soil erosion and runoff model. The value of Manning's n was based on Chow (1959). Table 1. shows the value of Manning's n assigned to each land use. Values of Manning's n were adapted from Paningbatan (2001). Slight adjustments on some of the Manning's n values were made in order to fit the needs of the model.

Table 1. Saturated hydraulic conductivity and Manning's n values for various land uses.

Land use	Saturated hydraulic conductivity (Mm/Hr.)	Manning's n
Forest	100.8	0.1
Brush	42.0	0.12
Grass	100.8	0.035
Very thin grass	33.0	0.03
Bare	0.6	0.025
River	0.0	0.04
Terrace	6.0	0.06
Trail	0.6	0.025
Urban	0.6	0.02

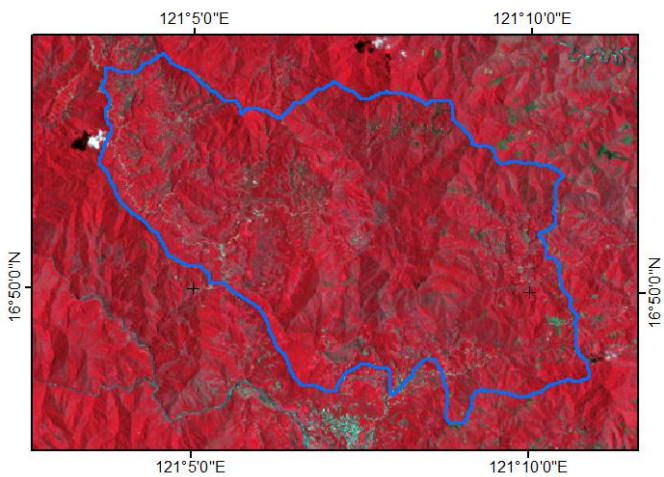

Fig. 3. Landsat 8 satellite data of Lagawe River Sub-watershed, Ifugao Province. Path 116, row 048, taken May 14, 2014. Watershed boundary is designated by the blue line.

The saturated hydraulic conductivity values used for various land uses is listed on Table 1. These values were recoded into the land use map and a saturated hydraulic conductivity map (Fig. 4i) was created for the sub-watershed. The values for saturated hydraulic of various land use/ land covers were taken from an unpublished thesis of Bato (1996) and adapted for use in this study. The model required the following maps and files as input (Fig. 4): (1) dem.map – DEM, (2) ldd.map – local drainage direction map, (3) slope.map – slope map, (4) station.map – water-level gauging station map, (5) rainstat.map – rain gauge station map, (6) mask.map – watershed boundary map, (7) mannings.map – Manning's Roughness Index Map, (8) landuse.map – land use map, (9) imap.map – hydraulic conductivity map, and (10) rain.tss – rainfall intensity time series text file. The model outputted the following maps and file: (1) zrun – surface runoff time series maps, (2) zsed – sediment time series map, and (3) runoff.tss – predicted water-level time series text file. All the input and output maps are

in raster format and share the same image dimension of rows: 246 and columns: 286 and an image resolution of 50 meters per pixel.

The model was written in ASCII format using PCRaster commands and syntax. The model code was divided into four parts: binding, timer, initial, and dynamic. The "binding" portion was where the input and output files were set. The "timer" portion was where the number of time-steps was set. Each time-step was equivalent to five seconds. The "initial" portion was the part of the model that created the static maps. The "dynamic" portion was the part of the model where iteration occurred, where time-series operations were performed, and where time-series maps and tables were created. Fig. 5 provides an overview of the model, the data inputs (maps and tabular data) and the data outputs (time-series maps, tabular data, and graphical streamflow data). All the maps shown in Fig. 4 and the tabular rainfall and water-level data are necessary to run the model.

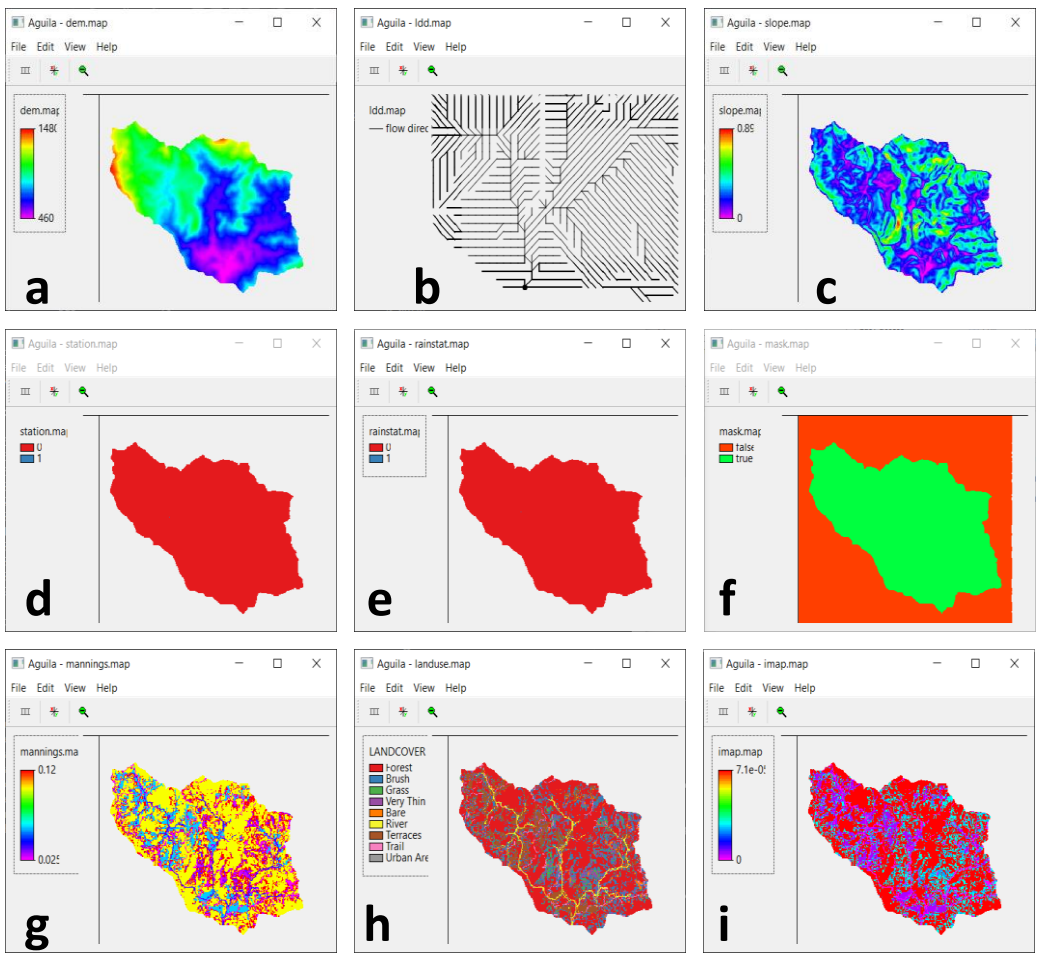

Fig. 4. Input maps required to run the model: (a) digital elevation model map, (b) local drainage direction map, (c) slope map, (d) water-level gauging station map, (e) rain gauge station map, (f) watershed boundary map, (g) Manning's Roughness Index Map, (h) land use map, and (i) infiltration capacity map.

The modified version of Manning's Equation (Equation 3) is operationalized in the model as shown in code snippet in Fig. 6. Surface runoff velocity is computed using Manning's Equation as shown in line 43 of the code snippet. The flux Q or volume of water discharge per unit time is computed in line 44. Because this section is "dynamic," the codes are run iteratively, based on the number of time-steps. Each time-step is equal to five seconds. The total number of time-steps depend on the duration of the rainstorm event. As the model runs, time-series maps are dynamically generated and the tabular runoff data is populated per time-step. At the end of the model run, the streamflow hydrograph is displayed.

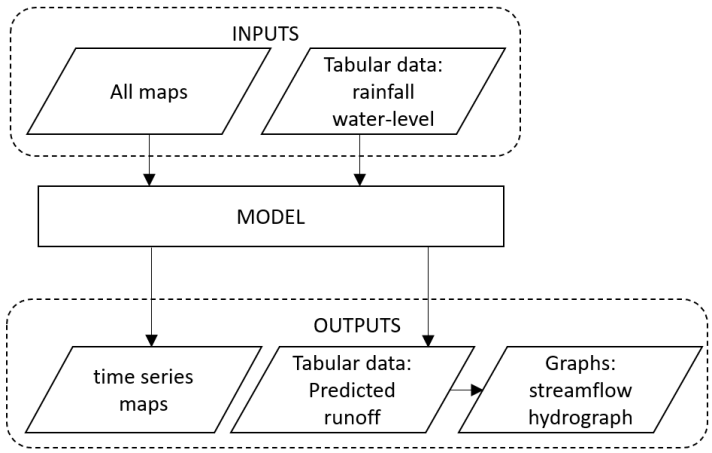

Fig. 5. Overview of the physically-based model for simulating runoff.

```
36 dynamic
37 RainWater = (timeinputscalar(RainTimeSeries, RainZones))/120;
38 RainWater2 = RainWater + SurfaceWater3;
39 InfDepth = min(RainWater2, iMap);
40 InfDepth2 = InfDepth2 + InfDepth;
41 SurfaceWater = max((RainWater2 - iMap),0.000001);
42 s = max((max(Slope, 0.01)**(0.50000)),0.000001);
43 Velocity = max((((SurfaceWater**(0.66667)) * s)/ ManningsMap),0.000001);
44 q = (Velocity *1.1*(SurfaceWater));
45 RunOff2 = q/50;
46 RunOff2a = upstream(Ldd, RunOff2);
47 report RunOffTot = max(((SurfaceWater + RunOff2a) - RunOff2), 0);
48 SurfaceWater2 = max(RunOffTot,0.000000001);
49 SurfaceWater3 = SurfaceWater2;
50 Runoff = ((SurfaceWater3 *50)/20)+0.45;
```

Fig. 6. Code snippet of the physically-based model for simulating runoff.

To determine how well the model performed in simulating surface runoff, correlation analysis, the Welch t-test, and Nash and Sutcliffe indices were used to evaluate the results.

Correlation was performed to determine the "goodness-of-fit" between the measured and predicted datasets. A good correlation should yield a high R^2 value close to 1.0. The correlation analysis was performed in Microsoft Excel 2019. The Welch t-test is a statistical test to determine if two sample means (measured and the predicted), with unequal variances, are statistically different. The null hypothesis of this statistical test is that there is no significant difference between the mean of the measured and the predicted. The alternative hypothesis is that there is a significant difference between

the mean of the measured and the predicted. For the null hypothesis to be accepted and the alternative hypothesis to be rejected, the p-value (probability value) should be above 0.05 (5% level of significance) and the t-statistic should be below 1.96. The Welch t-test was performed using R Software version 3.6.2.

The Nash and Sutcliffe (NSE) is an index of model performance. An NSE value of one indicates a perfect prediction; a negative value indicates a less than-reliable prediction. A negative NSE value also means that the sample mean is much better predictor than the model. The NSE index is computed using Equation 6.

$$NSE = 1 - \frac{\sum_{i=1}^{n}\left(X_{mi} - X_{pi}\right)^2}{\sum_{i=i}^{n}(X_{mi} - \bar{X}_m)^2}$$

Where:

E is the efficiency of the model *(Eq. 6)*

X_{mi} is the measured value

X_{pi} is the predicted value

$\bar{X}_m$ is the mean of the measured values

RESULTS AND DISCUSSION

Four erosive rainstorm events were considered among the entire set of rainfall data gathered. Other rainfall events that were deemed non-erosive due their low intensity and short duration were not included in the analysis. Data from individual rainstorm events were lumped together for correlation analysis. Fig.7 shows the overall correlation between the measured and the predicted streamflow. The best-fit line has an R^2 of 0.82, indicating a linearly positive relationship. This high R^2 value is supported visually by the similarity in the shape of the measured and predicted streamflow curves in Fig. 8 for individual rainstorm events. The Welch Two Sample t-test yielded a t-statistic of 1.76, a probability value of 0.08, and 558.51 degrees of freedom. The critical t-value at 5% level of significance is 1.96, which is greater than the t-statistic value of 1.76. The probability value of 0.08 is also greater than 0.05 (5%) level of significance. The results of the physical model is significant, and the statistical test is in favor of the null hypothesis and rejection of the alternative hypothesis: the physical, dynamic model is able to simulate streamflow without any significant difference from the measured streamflow of Lagawe River Sub-watershed.

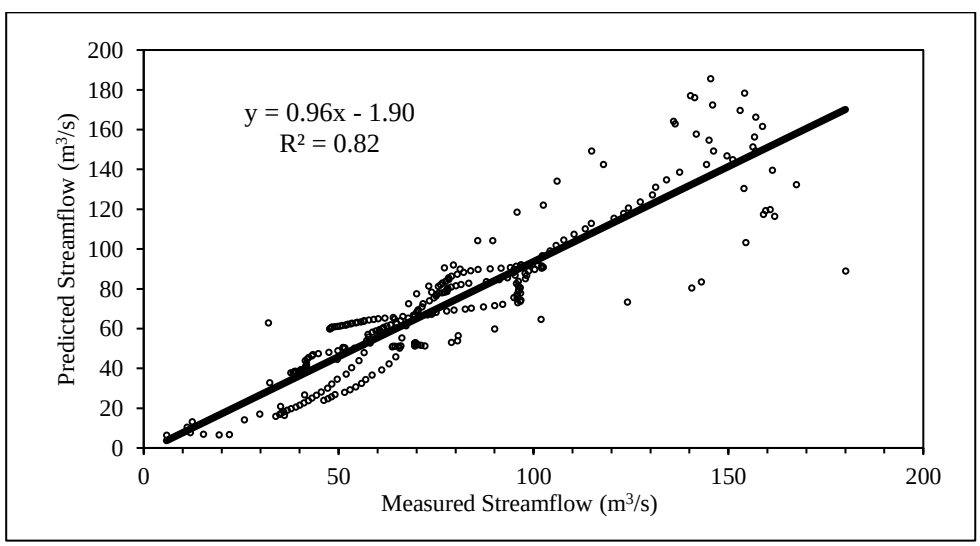

Fig. 7. Correlation analysis of measured and predicted streamflow, Lagawe River.

Table 2 shows the goodness-of-fit indices of streamflow curves for four rainstorm events in 2015.

Table 2. Goodness of fit indices of streamflow curves for various rainstorm events.

Event No.	Date	R^2	NSE
1	May 12-13, 2015	0.84	0.74
2	August 18, 2015	0.74	0.62
3	October 18-19, 2015	0.79	0.74
4	December 16, 2015	0.95	0.95

Figure 8 shows the predicted and measured streamflow curves for the Lagawe River for individual rainstorm events, together with rainfall intensity and depth. Rainstorm event 1 (Fig. 8a), with a rainfall depth of 37 mm., a rainfall duration of 3 hours, and a maximum intensity of 49 mm/hr., generated a maximum streamflow of about 160 m^3/s, with a lag time of about 2 hours. Regression analysis of the measured and predicted streamflow generated an R^2 of 0.84 (Table 2), indicating that the model has a predicting precision of 84% in the case of this rainstorm event. The NSE (Nash and Sutcliffe, 1970) coefficient is 0.74, indicating that the model performed well in predicting streamflow for this rainstorm event. An NSE value of equal to one indicates a perfect prediction; a negative value indicates that the prediction is less reliable than using the sample mean.

The total volume of rainfall that fell within the watershed boundary for event 1 is 2,756,000 m^3. This rainstorm generated an estimated total surface runoff volume of 122,000 m^3, which eventually flowed to the Magat River Reservoir. This stored water will be utilized for hydroelectric power generation and irrigation.

Rainstorm event 2 (Fig. 8b), with a rainfall depth of 31 mm., a rainfall duration of 1½ hours, and a maximum intensity of 50 mm/hr., generated a maximum streamflow of about 180 m^3/s, with a lag time of about 1.5 hours. Regression analysis yielded an R^2 of 0.74, indicating that the model has a predicting precision of 74% in the case of this rainstorm event. The NSE coefficient is 0.64, indicating that the model performed modestly in predicting streamflow for this rainstorm event.

The total volume of rainfall that fell within the watershed boundary for event 2 is 2,309,000 m^3, which generated an estimated total surface runoff volume of 95,000 m^3.

Rainstorm event 3 (Fig. 8c) occurred during the onslaught of Super Typhoon Lando (International Name: Koppu) in the Philippines and brought extreme rainfall from October 14-21, 2015 (NASA 2015; NDRRMC 2015). Rainstorm event 3 generated a rainfall depth of 68 mm, a rainfall duration of 7 hours, and a maximum intensity of 41 mm/hr. A maximum streamflow of about 160 m^3/s was reached, with a lag time of about 1.5 hours. Regression analysis yielded an R^2 of 0.79, indicating that the model has a predicting precision of 79% in the case of this rainstorm event. The NSE coefficient is 0.74, indicating that the model performed well in predicting streamflow for this rainstorm event.

The total volume of rainfall that fell within the watershed boundary is 5,041,000 m^3. This rainstorm generated an estimated total surface runoff volume of 422,000 m^3. Rainstorm events with high intensity and long duration, such as Rainstorm event 3, generated a high volume of rainfall, which in turn generated a large volume of surface runoff.

Rainstorm event 4 (Fig. 8d), with a rainfall depth of 75 mm, a rainfall duration of 18 hours, and a maximum intensity of 9.2 mm/hr., generated a maximum streamflow of 105 m^3/s. Regression analysis yielded an R^2 of 0.95, indicating that the model has a predicting precision of 95% in the case

of this rainstorm event. The NSE coefficient is 0.95, indicating that the model performed very well in predicting streamflow for this rainstorm event.

A total of 5,578,000 m^3 of rainfall fell within the watershed boundary for event 4, which generated an estimated total surface runoff of 381,000 m^3.

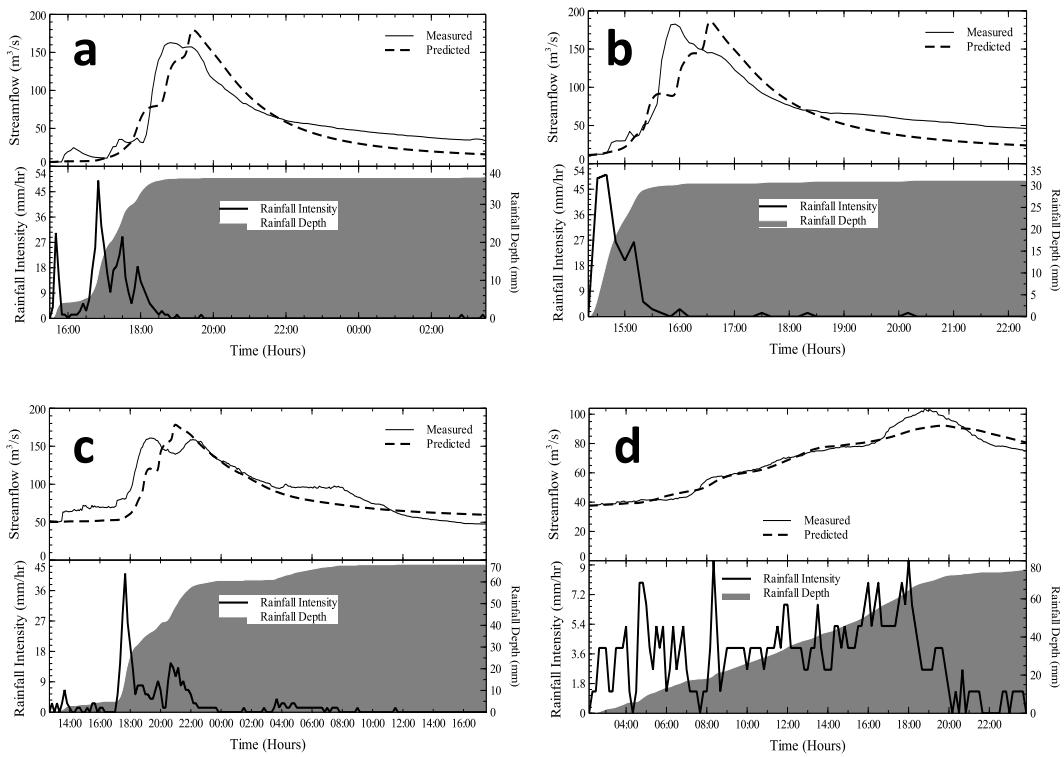

Fig. 8. Measured and predicted streamflow of Lagawe River and rainfall intensity and depth, (a) May 12-13, 2015, (b) August 18, 2015, (c) October 18-19, 2015, and (d) December 16, 2015.

CONCLUSION

A dynamic, physical model that can simulate runoff and streamflow during rainstorm events using GIS, remote sensing, and sensor technologies have been developed. For the model to work and to be operationalized, two data must be present. First is the satellite-based land use/land cover map and the second is the event-based rainfall data. A satellite-based land use/ land cover map as a product of an image classification process ensures that the most recent land use condition is reflected on the model. This land use map shows the true condition of the landscape on the ground and will be used as the surrogate date for Manning's Roughness Coefficient and the infiltration capacity.

Event-based rainfall data is also very much needed by the model. Experience shows that daily rainfall statistics is of less value as it does not show the varying intensities of rainfall as time progresses and does not provide information on the duration of the rainfall or the number of rainfall episodes that occur within a day.

Manning's Equation is normally used by hydrologic engineers to compute for the flow velocity and volume discharge of rivers. This study demonstrates clearly Manning's Equation's use to model

the flow of water across a landscape, with various land uses/ land covers as surface runoff. The flow of surface runoff follows the local drainage divide of the watershed and will eventually converge at the main channel of the river, where Manning's Equation will again be used to compute for flow velocity and volume. Thus, the use of Manning's Equation is not limited to river channels, but can also be adapted for surface flow, with uniform slope.

ACKNOWLEDGEMENT

The authors are grateful for the technical guidance provided by Dr. Rex Victor O. Cruz, Dr. Victor B. Ella, and Dr. Pearl B. Sanchez during the conduct of this research. The authors would also like to thank Dr. Elpidio L. Rosario and Dr. Eduardo C. Sison of the Madecor Group of Companies, Philippines, for allowing the use of rainfall and water-level data for this research.

REFERENCES CITED

Bato, V. A. 1996. The relationship of earthworm population with some soil physical properties of Lipa soil series. BS Thesis, University of the Philippines Los Banos. University of the Philippines Los Banos Library, Laguna, Philippines.

Bato, V. A. 2019. Developing a dynamic model to predict soil erosion and runoff in a watershed. PhD Dissertation, University of the Philippines, Los Banos. University of the Philippines Los Banos Library, Laguna, Philippines.

Besaw, L. E., Rizzo, D. M., Bierman, P. R. and W. R. Hackett. 2010. Advances in ungauged streamflow prediction using artificial neural networks. Journal of Hydrology. 386(1-4): 27-37.

Chow, V. T. 1959. Open-channel hydraulics. McGraw-Hill. New York, USA. 680p.

FAO [Food and Agriculture Organization]. n.d. Sustainable Forest Management (SFM) Toolbox. Retrieved January 6, 2020 from http://www.fao.org/sustainable-forest-management/toolbox/modules/watershed-management/basic-knowledge/en/.

FMB [Forest Management Bureau]. n.d. Watershed characterization and vulnerability assessment using gis and remote sensing. Department of Environment and Natural Resources. Forest Management Bureau. Retrieved May 31, 2019 from https://forestry.denr.gov.ph/pdf/ref/wcvagis.pdf.

Frisbee, M. D., Phillips, F. M., Campbell, A. R., Liu, F. and S. A. Sanchez. 2011. Streamflow generation in a large, alpine watershed in the southern Rocky Mountains of Colorado: Is streamflow generation simply the aggregation of hill slope runoff responses? Water Resources Research. 47(6):1-8.

He, Z., Wen, X., Liu, H. and J. Du. 2014. A comparative study of artificial neural network, adaptive neuro fuzzy inference system and support vector machine for forecasting river flow in the semiarid mountain region. Journal of Hydrology. 509:379-386.

Hillel, D. 2004. Introduction to Environmental Soil Physics. Elsevier Science USA. 494 p.

Kuchment, L. S., Demidov, V. N. and D. M. Cooper. 1996. Rainfall-runoff modelling of the Ouse basin, North Yorkshire: an application of a physically distributed model. Journal of Hydrology. 181(1-4): 323-342.

Mehr, A. D., Kayha, E. and E. Olyaie. 2013. Streamflow prediction using linear genetic programming in comparison with neuro-wavelet technique. Journal of Hydrology. 505:240-249.

NASA. [National Aeronautics and Space Administration]. 2015. Koppu (NW Pacific). Retrieved January 10, 2020 from https://www.nasa.gov/feature/goddard/koppu-nw-pacific.

Nash, J. E. and J. V. Sutcliffe. 1970. River flow forecasting through conceptual models part I – A discussion of principles. Journal of Hydrology. 10(3): 282-290.

NDRRMC. [National Disaster Risk Reduction & Management Council] 2015. SitRep No. 22 re Preparedness measures and effects of Typhoon "Lando" (I.N. KOPPU). Retrieved January 20, 2020 from http://www.ndrrmc.gov.ph/attachments/article/2607/SitRep%20No.22%20re%20Preparedness%20Measures%20and%20Effects%20of%20Typhoon%20LANDO%20(I.N.%20KOPPU).pdf. 33 p.

Pandey, A., Chowdary, V. M., Mal, B. C. and M. Billib. 2008. Runoff and sediment yield modeling from a small agricultural watershed in India using the WEPP model. Journal of Hydrology. 348 (3-4): 305-319.

Paningbatan Jr., E. P. 2001. Geographic information system-assisted dynamic modelling of soil erosion and hydrologic processes at a watershed scale. The Philippine Agricultural Scientist. 84: 388-393.

Postel, S. L. and B. H. Thompson Jr. 2005. Watershed protection: Capturing the benefits of nature's water supply service. Natural Resources Forum. 29: 98-108. doi:10.1111/j.1477-8947.2005.00119.x.

Razavi, T. and P. Coulibaly. 2013. Streamflow prediction in ungauged basins: Review of regionalization methods. Journal of Hydrologic Engineering. 18(8):958-975.

Tu, J. 2009. Combined impact of climate and land use change on streamflow and water quality in eastern Massachusetts, USA. Journal of Hydrology. 379 (3-4):268-283.

Wiche, G. J. and R.R. Holmes Jr. 2016. Streamflow Data, pp 371-398. In Adams III, T. E, and Pagano, T. C. (Eds.). Flood Forecasting A Global Perspective. Elsevier Inc. USA.

Wu, C. L. and K. W. Chau. 2011. Rainfall-runoff modeling using artificial neural network coupled with singular spectrum analysis. Journal of Hydrology. 399 (3-4): 394-409.

Wu, L., Jiang, J., Li, G. and X. Ma. 2018. Characteristics of pulsed runoff-erosion events under typical rainstorms in a small watershed on the Loess Plateau of China. Scientific Reports. 8: 1-12. doi:10.1038/s41598-018-22045-x.

Yan, B., Fang, N. F., Zhang, P. C. and Z. H. Shi. 2013. Impacts of land use change on watershed streamflow and sediment yield: An assessment using hydrologic modelling and partial least squares regression. Journal of Hydrology. 484: 26-37.